Supporting Information

Insight into spodium–π bonding characteristics of the $MX_2\cdots\pi$ (M = Zn, Cd and Hg; X = Cl, Br and I) complexes– A theoretical study

Meng Gao [1,*], Qibo Zhao [1], Hao Yu [1], Min Fu [1], and Qingzhong Li [2,*]

[1] College of Chemical and Biological Engineering, Shandong University of Science and Technology, Qingdao 266590, China;

[2] The Laboratory of Theoretical and Computational Chemistry, School of Chemistry and Chemical Engineering, Yantai University, Yantai 264005, China

* Corresponding Authors: Meng Gao, E-mail: skd996370@sdust.edu.cn; Qingzhong Li, E-mail: li70316@sohu.com.

Table S1. Distances (R, Å) between M in MX_2 and the centers of C–C bond in π molecules (* denote the centers of C–C bond), angles of X-M-X in MX_2 (α, deg), dihedral angle of X–X···C–C (θ, deg), and interaction energy (ΔE, kcal/mol) in the complexes at the MP2/aug-cc-pVTZ level.

	$R_{M\cdots*}$	$R_{M\text{-}X}$	$R_{C\text{-}C}$	α	θ	ΔE
$ZnCl_2\cdots C_2H_2$–P	2.406	2.094	1.218	151	0	–11.60
$ZnBr_2\cdots C_2H_2$–P	2.387	2.222	1.219	149	0	–9.72
$ZnI_2\cdots C_2H_2$–P	2.387	2.411	1.220	146	0	–8.30
$CdCl_2\cdots C_2H_2$–P	2.664	2.280	1.218	163	0	–9.66
$CdBr_2\cdots C_2H_2$–P	2.670	2.401	1.218	161	0	–8.26
$CdI_2\cdots C_2H_2$–P	2.700	2.580	1.218	159	0	–6.82
$HgCl_2\cdots C_2H_2$–P	3.056	2.238	1.215	176	0	–3.92
$HgBr_2\cdots C_2H_2$–P	3.078	2.363	1.215	175	0	–2.96
$HgI_2\cdots C_2H_2$–P	3.145	2.541	1.215	175	0	–2.11
$ZnCl_2\cdots C_2H_2$–T	2.545	2.077	1.216	159	83	–6.26
$ZnBr_2\cdots C_2H_2$–T	2.538	2.204	1.216	158	83	–5.29
$ZnI_2\cdots C_2H_2$–T	2.575	2.391	1.216	157	83	–4.76
$CdCl_2\cdots C_2H_2$–T	2.757	2.268	1.216	166	83	–6.11
$CdBr_2\cdots C_2H_2$–T	2.770	2.389	1.216	165	83	–5.24
$CdI_2\cdots C_2H_2$–T	2.806	2.566	1.216	165	83	–4.31
$HgCl_2\cdots C_2H_2$–T	3.083	2.234	1.214	177	84	–2.30
$HgBr_2\cdots C_2H_2$–T	3.081	2.359	1.214	176	84	–1.78
$HgI_2\cdots C_2H_2$–T	3.127	2.541	1.214	176	83	–1.37
$ZnCl_2\cdots C_2H_4$–P	2.391	2.090	1.346	148	0	–11.68
$ZnBr_2\cdots C_2H_4$–P	2.367	2.225	1.347	146	0	–10.89
$ZnI_2\cdots C_2H_4$–P	2.361	2.414	1.348	143	0	–9.78
$CdCl_2\cdots C_2H_4$–P	/	/	/	/	/	/
$CdBr_2\cdots C_2H_4$–P	2.635	2.406	1.344	157	0	–8.58
$CdI_2\cdots C_2H_4$–P	2.649	2.584	1.345	155	0	–7.26
$HgCl_2\cdots C_2H_4$–P	/	/	/	/	/	/
$HgBr_2\cdots C_2H_4$–P	3.051	2.364	1.338	174	0	–2.12
$HgI_2\cdots C_2H_4$–P	3.090	2.542	1.338	173	0	–1.40
$ZnCl_2\cdots C_2H_4$–T	2.410	2.089	1.346	155	82	–11.09
$ZnBr_2\cdots C_2H_4$–T	2.400	2.216	1.346	153	82	–9.51

$ZnI_2\cdots C_2H_4$–T	2.409	2.405	1.346	152	82	–7.87
$CdCl_2\cdots C_2H_4$–T	2.637	2.279	1.344	163	82	–9.52
$CdBr_2\cdots C_2H_4$–T	2.640	2.401	1.344	163	82	–8.17
$CdI_2\cdots C_2H_4$–T	2.664	2.578	1.344	162	82	–6.80
$HgCl_2\cdots C_2H_4$–T	2.934	2.241	1.339	175	82	–3.32
$HgBr_2\cdots C_2H_4$–T	2.924	2.365	1.339	175	82	–2.30
$HgI_2\cdots C_2H_4$–T	2.949	2.543	1.339	174	82	–1.60
$ZnCl_2\cdots C_2F_2$–P	2.869	2.058	1.199	171	33	–2.36
$ZnBr_2\cdots C_2F_2$–P	2.886	2.184	1.199	171	42	–1.26
$ZnI_2\cdots C_2F_2$–P	2.958	2.372	1.198	172	50	–1.36
$CdCl_2\cdots C_2F_2$–P	2.957	2.255	1.200	173	33	–3.25
$CdBr_2\cdots C_2F_2$–P	2.976	2.376	1.199	174	40	–2.39
$CdI_2\cdots C_2F_2$–P	3.026	2.554	1.199	174	47	–1.77
$HgCl_2\cdots C_2F_2$–P	3.162	2.230	1.197	179	39	–1.64
$HgBr_2\cdots C_2F_2$–P	3.152	2.355	1.197	179	46	–1.03
$HgI_2\cdots C_2F_2$–P	3.177	2.533	1.197	179	52	–0.79
$ZnCl_2\cdots C_2Li_2$–P	1.965	2.222	1.277	120	0	–106.75
$ZnBr_2\cdots C_2Li_2$–P	1.968	2.348	1.276	119	0	–99.94
$ZnI_2\cdots C_2Li_2$–P	1.976	2.535	1.276	117	1	–93.57
$CdCl_2\cdots C_2Li_2$–P	2.166	2.421	1.279	134	0	–97.43
$CdBr_2\cdots C_2Li_2$–P	2.172	2.534	1.279	132	0	–89.97
$CdI_2\cdots C_2Li_2$–P	2.180	2.709	1.278	128	0	–83.63
$HgCl_2\cdots C_2Li_2$–P	2.141	2.439	1.291	129	0	–96.58
$HgBr_2\cdots C_2Li_2$–P	2.152	2.543	1.289	126	0	–87.51
$HgI_2\cdots C_2Li_2$–P	2.167	2.699	1.287	123	0	–78.82

Table S2. Charge transfer (CT, e), Second-order perturbation energies ($E^{(2)}$, kcal/mol) and Wiberg bond index (WBI) in the complexes at the HF/aug-cc-pVTZ level.

	CT	$E^{(2)}$	WBI
$ZnCl_2\cdots C_2H_2$–P	–0.067	35.25	0.1018
$ZnBr_2\cdots C_2H_2$–P	–0.073	46.63	0.1108
$ZnI_2\cdots C_2H_2$–P	–0.074	39.06	0.1149
$CdCl_2\cdots C_2H_2$–P	–0.061	24.99	0.0690
$CdBr_2\cdots C_2H_2$–P	–0.067	27.38	0.0738
$CdI_2\cdots C_2H_2$–P	–0.068	27.80	0.0752
$HgCl_2\cdots C_2H_2$–P	–0.022	7.58	0.0280
$HgBr_2\cdots C_2H_2$–P	–0.024	8.63	0.0309
$HgI_2\cdots C_2H_2$–P	–0.023	8.19	0.0317
$ZnCl_2\cdots C_2H_2$–T	–0.063	30.70	0.0823
$ZnBr_2\cdots C_2H_2$–T	–0.071	34.32	0.0760
$ZnI_2\cdots C_2H_2$–T	–0.074	31.94	0.0701
$CdCl_2\cdots C_2H_2$–T	–0.060	20.95	0.0571
$CdBr_2\cdots C_2H_2$–T	–0.067	22.56	0.0612
$CdI_2\cdots C_2H_2$–T	–0.069	22.14	0.0615
$HgCl_2\cdots C_2H_2$–T	–0.025	7.62	0.0271
$HgBr_2\cdots C_2H_2$–T	–0.030	8.78	0.0309
$HgI_2\cdots C_2H_2$–T	–0.033	9.50	0.0331
$ZnCl_2\cdots C_2H_4$–P	–0.078	27.50	0.0920
$ZnBr_2\cdots C_2H_4$–P	–0.082	44.90	0.0996
$ZnI_2\cdots C_2H_4$–P	–0.083	57.23	0.1044
$CdCl_2\cdots C_2H_4$–P	/	/	/
$CdBr_2\cdots C_2H_4$–P	–0.098	31.43	0.0981
$CdI_2\cdots C_2H_4$–P	–0.099	33.48	0.0999
$HgCl_2\cdots C_2H_4$–P	/	/	/
$HgBr_2\cdots C_2H_4$–P	–0.039	12.95	0.0438
$HgI_2\cdots C_2H_4$–P	–0.040	13.40	0.0450
$ZnCl_2\cdots C_2H_4$–T	–0.085	44.95	0.0851
$ZnBr_2\cdots C_2H_4$–T	–0.093	48.67	0.0907
$ZnI_2\cdots C_2H_4$–T	–0.100	58.39	0.0934
$CdCl_2\cdots C_2H_4$–T	–0.095	27.99	0.0883
$CdBr_2\cdots C_2H_4$–T	–0.102	30.13	0.0922

$CdI_2\cdots C_2H_4$–T	–0.106	31.59	0.0923
$HgCl_2\cdots C_2H_4$–T	–0.048	14.69	0.0484
$HgBr_2\cdots C_2H_4$–T	–0.055	17.06	0.0539
$HgI_2\cdots C_2H_4$–T	–0.059	17.98	0.0556
$ZnCl_2\cdots C_2F_2$–P	–0.039	15.43	0.0412
$ZnBr_2\cdots C_2F_2$–P	–0.042	17.84	0.0433
$ZnI_2\cdots C_2F_2$–P	–0.041	18.9	0.0407
$CdCl_2\cdots C_2F_2$–P	–0.040	13.89	0.0414
$CdBr_2\cdots C_2F_2$–P	–0.043	15.31	0.0430
$CdI_2\cdots C_2F_2$–P	–0.042	15.88	0.0436
$HgCl_2\cdots C_2F_2$–P	–0.020	7.07	0.0231
$HgBr_2\cdots C_2F_2$–P	–0.024	8.93	0.0267
$HgI_2\cdots C_2F_2$–P	–0.026	10.53	0.0290
$ZnCl_2\cdots C_2Li_2$–P	–0.907	128.48	0.2540
$ZnBr_2\cdots C_2Li_2$–P	–1.043	61.84	0.2619
$ZnI_2\cdots C_2Li_2$–P	–0.870	24.99	0.2758
$CdCl_2\cdots C_2Li_2$–P	–1.090	113.82	0.2967
$CdBr_2\cdots C_2Li_2$–P	–1.094	110.02	0.3052
$CdI_2\cdots C_2Li_2$–P	–1.055	107.76	0.3098
$HgCl_2\cdots C_2Li_2$–P	–1.293	48.5(91.98)[a]	0.3873
$HgBr_2\cdots C_2Li_2$–P	–1.157	183.55	0.3881
$HgI_2\cdots C_2Li_2$–P	–1.040	171.21	0.3876

Note: The charge transfer is the sum of atomic charge of the MX_2 in the complexes. $E^{(2)}$ is the stabilization energy due to the orbital interactions of $BD_{C=C/C\equiv C}\rightarrow LP^*_M$. [a] the value in the parentheses is the stabilization energy due to the orbital interactions of $BD_{C-Li}\rightarrow LP^*_M$. WBI values correspond to the M···C in the complexes.

Table S3. Electron density (ρ, au), Laplacian ($\nabla^2\rho$, au), and total energy density (*H*, au) at the intermolecular bond critical points (BCPs) in the complexes at the MP2/aug-cc-pVTZ level.

	ρ	$\nabla^2\rho$	*H*
$ZnCl_2\cdots C_2H_2$–P	0.0384	0.0988	–0.0070
$ZnBr_2\cdots C_2H_2$–P	0.0398	0.1023	–0.0076
$ZnI_2\cdots C_2H_2$–P	0.0400	0.1018	–0.0077
$CdCl_2\cdots C_2H_2$–P	0.0295	0.0875	–0.0018
$CdBr_2\cdots C_2H_2$–P	0.0292	0.0863	–0.0018
$CdI_2\cdots C_2H_2$–P	0.0276	0.0812	–0.0014
$HgCl_2\cdots C_2H_2$–P	0.0166	0.0499	0.0008
$HgBr_2\cdots C_2H_2$–P	0.0160	0.0480	0.0009
$HgI_2\cdots C_2H_2$–P	0.0141	0.0427	0.0010
$ZnCl_2\cdots C_2H_2$–T	0.0292	0.0747	–0.0036
$ZnBr_2\cdots C_2H_2$–T	0.0297	0.0754	–0.0037
$ZnI_2\cdots C_2H_2$–T	0.0283	0.0711	–0.0033
$CdCl_2\cdots C_2H_2$–T	0.0245	0.0722	–0.0006
$CdBr_2\cdots C_2H_2$–T	0.0242	0.0708	–0.0006
$CdI_2\cdots C_2H_2$–T	0.0226	0.0655	–0.0003
$HgCl_2\cdots C_2H_2$–T	0.0159	0.0473	0.0009
$HgBr_2\cdots C_2H_2$–T	0.0157	0.0468	0.0009
$HgI_2\cdots C_2H_2$–T	0.0147	0.0438	0.0010
$ZnCl_2\cdots C_2H_4$–P	0.0402	0.0857	–0.0083
$ZnBr_2\cdots C_2H_4$–P	0.0421	0.0893	–0.0091
$ZnI_2\cdots C_2H_4$–P	0.0426	0.0898	–0.0094
$CdCl_2\cdots C_2H_4$–P	/	/	/
$CdBr_2\cdots C_2H_4$–P	0.0319	0.0817	–0.0030
$CdI_2\cdots C_2H_4$–P	0.0311	0.0793	–0.0028
$HgCl_2\cdots C_2H_4$–P	/	/	/
$HgBr_2\cdots C_2H_4$–P	0.0175	0.0463	0.0005
$HgI_2\cdots C_2H_4$–P	0.0163	0.0434	0.0006
$ZnCl_2\cdots C_2H_4$–T	0.0385	0.0832	–0.0075
$ZnBr_2\cdots C_2H_4$–T	0.0393	0.0843	–0.0078
$ZnI_2\cdots C_2H_4$–T	0.0388	0.0821	–0.0077

$CdCl_2\cdots C_2H_4$–T	0.0316	0.0814	–0.0028
$CdBr_2\cdots C_2H_4$–T	0.0315	0.0807	–0.0028
$CdI_2\cdots C_2H_4$–T	0.0302	0.0770	–0.0025
$HgCl_2\cdots C_2H_4$–T	0.0215	0.0561	–0.0002
$HgBr_2\cdots C_2H_4$–T	0.0220	0.0570	–0.0003
$HgI_2\cdots C_2H_4$–T	0.0211	0.0547	–0.0001
$ZnCl_2\cdots C_2F_2$–P	0.0162	0.0426	0.0000
$ZnBr_2\cdots C_2F_2$–P	0.0158	0.0412	0.0001
$ZnI_2\cdots C_2F_2$–P	0.0140	0.0363	0.0003
$CdCl_2\cdots C_2F_2$–P	0.0173	0.0506	0.0005
$CdBr_2\cdots C_2F_2$–P	0.0168	0.0486	0.0005
$CdI_2\cdots C_2F_2$–P	0.0154	0.0440	0.0006
$HgCl_2\cdots C_2F_2$–P	0.0143	0.0430	0.0010
$HgBr_2\cdots C_2F_2$–P	0.0140	0.0423	0.0010
$HgI_2\cdots C_2F_2$–P	0.0138	0.0413	0.0010
$ZnCl_2\cdots C_2Li_2$–P	0.0882	0.2278	–0.0312
$ZnBr_2\cdots C_2Li_2$–P	0.0878	0.2251	–0.0309
$ZnI_2\cdots C_2Li_2$–P	0.0867	0.2204	–0.0303
$CdCl_2\cdots C_2Li_2$–P	0.0746	0.2134	–0.0192
$CdBr_2\cdots C_2Li_2$–P	0.0738	0.2095	–0.0189
$CdI_2\cdots C_2Li_2$–P	0.0729	0.2050	–0.0185
$HgCl_2\cdots C_2Li_2$–P	0.0883	0.2272	–0.0261
$HgBr_2\cdots C_2Li_2$–P	0.0869	0.2212	–0.0255
$HgI_2\cdots C_2Li_2$–P	0.0849	0.2132	–0.0245

Table S4. Electrostatic energy (ES), exchange energy (EX), repulsion energy (REP), polarization energy (POL), and dispersion energy (DISP) in the selected complexes at the MP2/aug-cc-pVTZ level. All are in kcal/mol.

	ES	EX	REP	POL	DISP
$ZnCl_2\cdots C_2H_2$–P	–29.51	–45.06	83.67	–16.43	–4.99
$ZnBr_2\cdots C_2H_2$–P	–31.95	–51.86	96.03	–18.31	–5.66
$ZnI_2\cdots C_2H_2$–P	–33.54	–58.16	106.98	–20.00	–6.13
$CdCl_2\cdots C_2H_2$–P	–22.82	–34.95	63.84	–11.36	–5.33
$CdBr_2\cdots C_2H_2$–P	–23.41	–38.14	69.28	–11.88	–5.65
$CdI_2\cdots C_2H_2$–P	–23.12	–40.43	72.75	–12.03	–5.80
$HgCl_2\cdots C_2H_2$–P	–10.79	–18.85	32.79	–3.95	–4.35
$HgBr_2\cdots C_2H_2$–P	–10.75	–20.25	35.06	–3.99	–4.70
$HgI_2\cdots C_2H_2$–P	–9.88	–20.48	35.07	–3.72	–4.97
$ZnCl_2\cdots C_2H_2$–T	–16.81	–30.52	55.49	–10.42	–5.00
$ZnBr_2\cdots C_2H_2$–T	–18.09	–34.58	62.46	–11.21	–5.46
$ZnI_2\cdots C_2H_2$–T	–18.26	–37.43	66.72	–11.32	–5.73
$CdCl_2\cdots C_2H_2$–T	–13.59	–25.14	45.28	–8.09	–5.36
$CdBr_2\cdots C_2H_2$–T	–14.02	–27.28	48.73	–8.27	–5.60
$CdI_2\cdots C_2H_2$–T	–13.76	–28.69	50.53	–8.00	–5.70
$HgCl_2\cdots C_2H_2$–T	–6.91	–15.60	26.93	–3.27	–4.78
$HgBr_2\cdots C_2H_2$–T	–7.14	–17.03	29.18	–3.34	–5.11
$HgI_2\cdots C_2H_2$–T	–7.14	–17.03	29.18	–3.34	–5.11
$ZnCl_2\cdots C_2H_4$–P	–30.23	–49.51	92.10	–18.56	–6.91
$ZnBr_2\cdots C_2H_4$–P	–33.38	–57.61	106.78	–20.80	–7.76
$ZnI_2\cdots C_2H_4$–P	–35.71	–65.34	120.17	–22.91	–8.38
$CdCl_2\cdots C_2H_4$–P	/	/	/	/	/
$CdBr_2\cdots C_2H_4$–P	–24.55	–43.50	79.30	–14.31	–7.45
$CdI_2\cdots C_2H_4$–P	–25.25	–47.68	86.04	–14.91	–7.73
$HgCl_2\cdots C_2H_4$–P	/	/	/	/	/
$HgBr_2\cdots C_2H_4$–P	–11.32	–24.16	41.93	–4.88	–6.11
$HgI_2\cdots C_2H_4$–P	–11.06	–25.67	44.00	–4.81	–6.52
$ZnCl_2\cdots C_2H_4$–T	–27.21	–44.05	82.25	–16.39	–6.56
$ZnBr_2\cdots C_2H_4$–T	–29.13	–49.86	92.49	–17.69	–7.18

$ZnI_2\cdots C_2H_4$–T	–30.19	–55.15	101.17	–18.76	–7.57
$CdCl_2\cdots C_2H_4$–T	–22.12	–36.78	67.86	–12.68	–6.95
$CdBr_2\cdots C_2H_4$–T	–22.86	–40.02	73.28	–13.14	–7.27
$CdI_2\cdots C_2H_4$–T	–23.00	–43.02	77.81	–13.28	–7.45
$HgCl_2\cdots C_2H_4$–T	–12.84	–25.36	44.94	–6.00	–6.24
$HgBr_2\cdots C_2H_4$–T	–13.64	–28.38	50.07	–6.44	–6.75
$HgI_2\cdots C_2H_4$–T	–13.47	–30.12	52.52	–6.40	–7.14
$ZnCl_2\cdots C_2F_2$–P	–6.91	–16.31	29.05	–4.12	–5.24
$ZnBr_2\cdots C_2F_2$–P	–7.24	–18.32	32.41	–4.09	–5.88
$ZnI_2\cdots C_2F_2$–P	–6.94	–19.01	33.17	–3.60	–6.30
$CdCl_2\cdots C_2F_2$–P	–6.60	–16.13	28.85	–4.32	–5.88
$CdBr_2\cdots C_2F_2$–P	–6.89	–17.67	31.40	–4.21	–6.34
$CdI_2\cdots C_2F_2$–P	–6.94	–18.76	32.97	–3.85	–6.71
$HgCl_2\cdots C_2F_2$–P	–3.99	–11.54	20.02	–2.08	–5.44
$HgBr_2\cdots C_2F_2$–P	–4.47	–13.30	23.02	–2.17	–6.04
$HgI_2\cdots C_2F_2$–P	–4.82	–14.77	25.39	–2.11	–6.58
$ZnCl_2\cdots C_2Li_2$–P	–176.29	–169.28	331.47	–83.85	–10.44
$ZnBr_2\cdots C_2Li_2$–P	–171.59	–175.81	340.82	–86.87	–10.41
$ZnI_2\cdots C_2Li_2$–P	–161.80	–182.77	347.82	–91.36	–9.94
$CdCl_2\cdots C_2Li_2$–P	–164.34	–163.47	319.89	–80.70	–11.66
$CdBr_2\cdots C_2Li_2$–P	–157.82	–166.35	322.57	–81.82	–11.45
$CdI_2\cdots C_2Li_2$–P	–148.17	–169.49	323.53	–83.97	–10.81
$HgCl_2\cdots C_2Li_2$–P	–177.93	–210.50	411.49	–119.31	–11.32
$HgBr_2\cdots C_2Li_2$–P	–169.45	–211.53	410.98	–118.60	–10.72
$HgI_2\cdots C_2Li_2$–P	–156.48	–211.24	405.84	–117.79	–9.73

M	X	R_{M-X}
Zn	Cl	2.047
Zn	Br	2.174
Zn	I	2.362
Cd	Cl	2.245
Cd	Br	2.366
Cd	I	2.545
Hg	Cl	2.226
Hg	Br	2.350
Hg	I	2.530

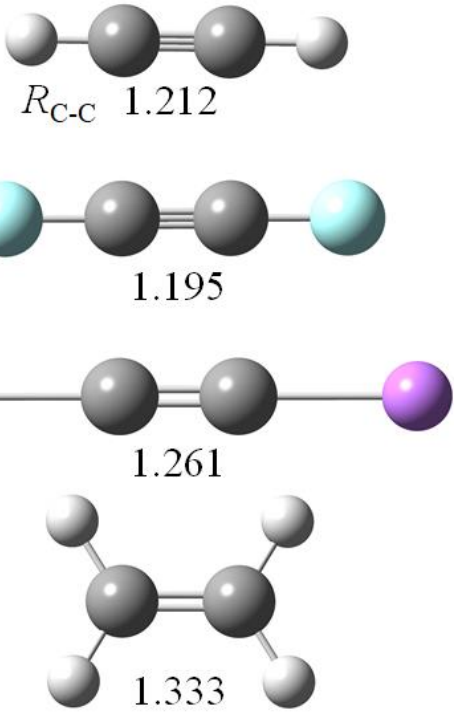

Figure S1. The optimized geometries of the MX_2 (M=Zn, Cd, Hg; X = Cl, Br, I), C_2H_2, C_2F_2, C_2Li_2 and C_2H_4 molecules at the MP2/aug-cc-pVTZ level.

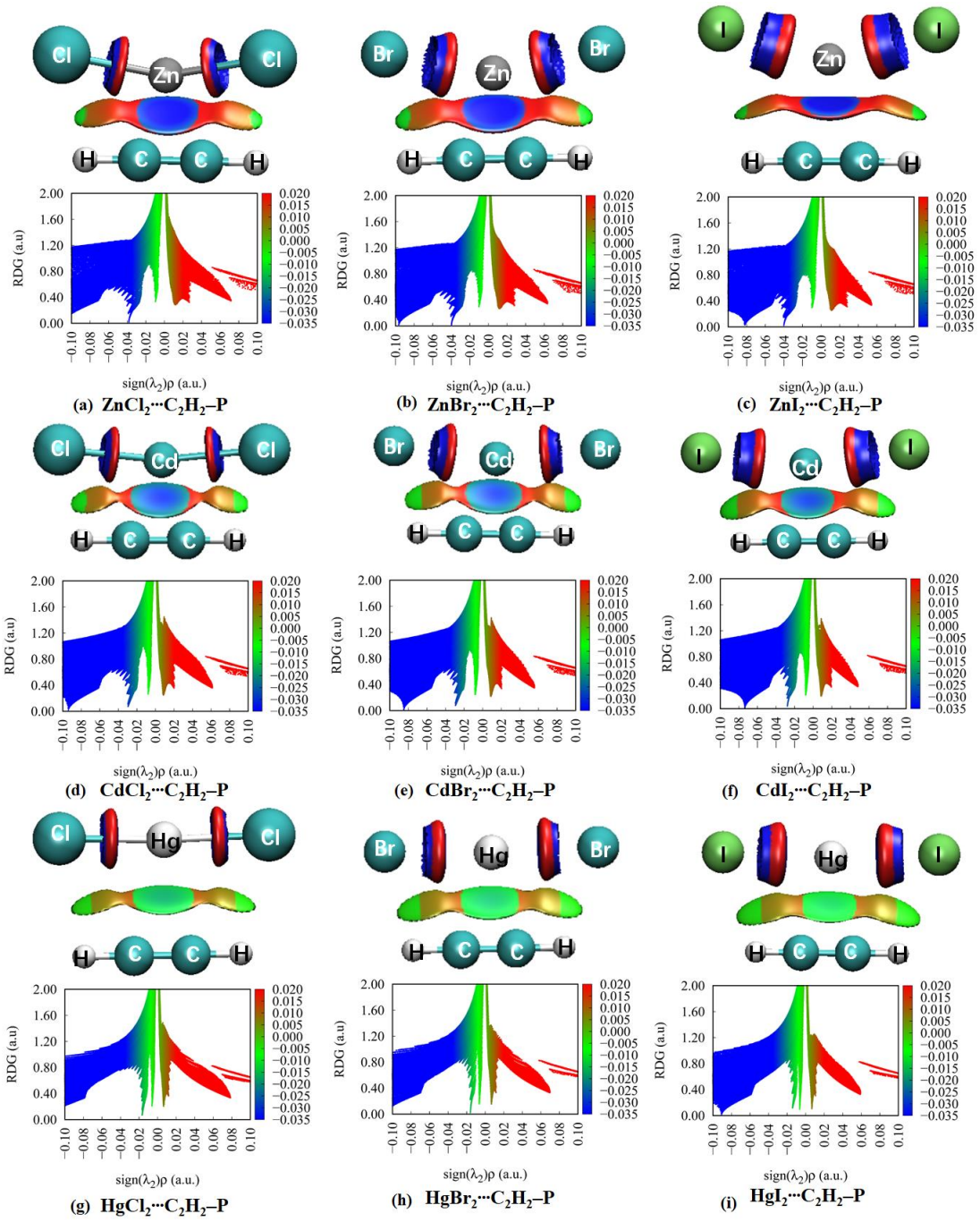

Figure S2. Plots of the reduced density gradient RDG *versus* the electron density multiplied by the sign of the second Hessian eigenvalue (sign(λ_2)ρ) of $MX_2\cdots C_2H_2$–P. NCI maps of the corresponding binary complexes. Blue, green, orange, and red areas correspond to strong attractive, weak attractive, weak repulsive, and strong repulsive interactions, respectively.

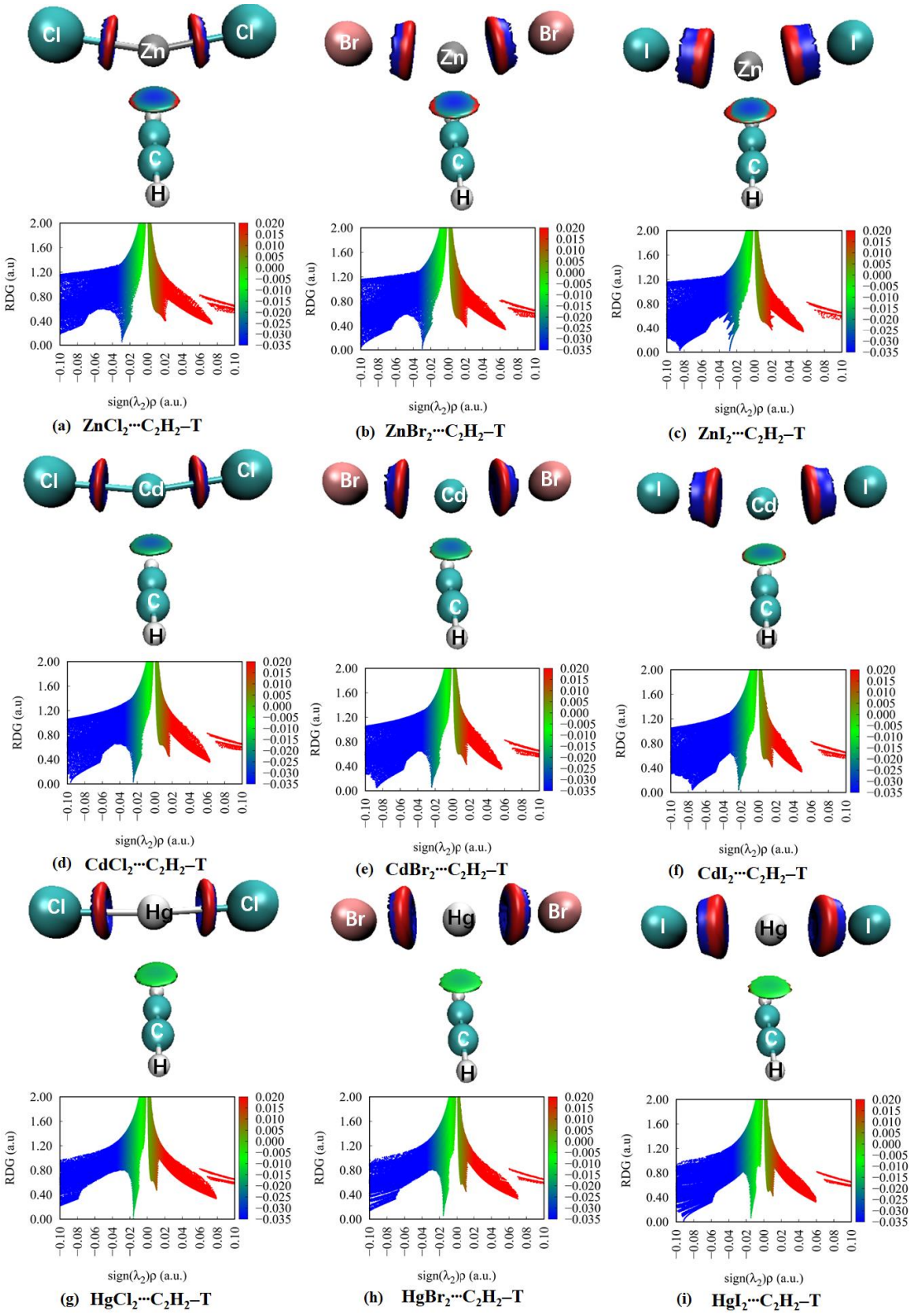

Figure S3. Plots of the reduced density gradient RDG *versus* the electron density multiplied by the sign of the second Hessian eigenvalue (sign(λ_2)ρ) of $MX_2\cdots C_2H_2$–T. NCI maps of the corresponding binary complexes. Blue, green, orange, and red areas correspond to strong attractive, weak attractive, weak repulsive, and strong repulsive interactions, respectively.

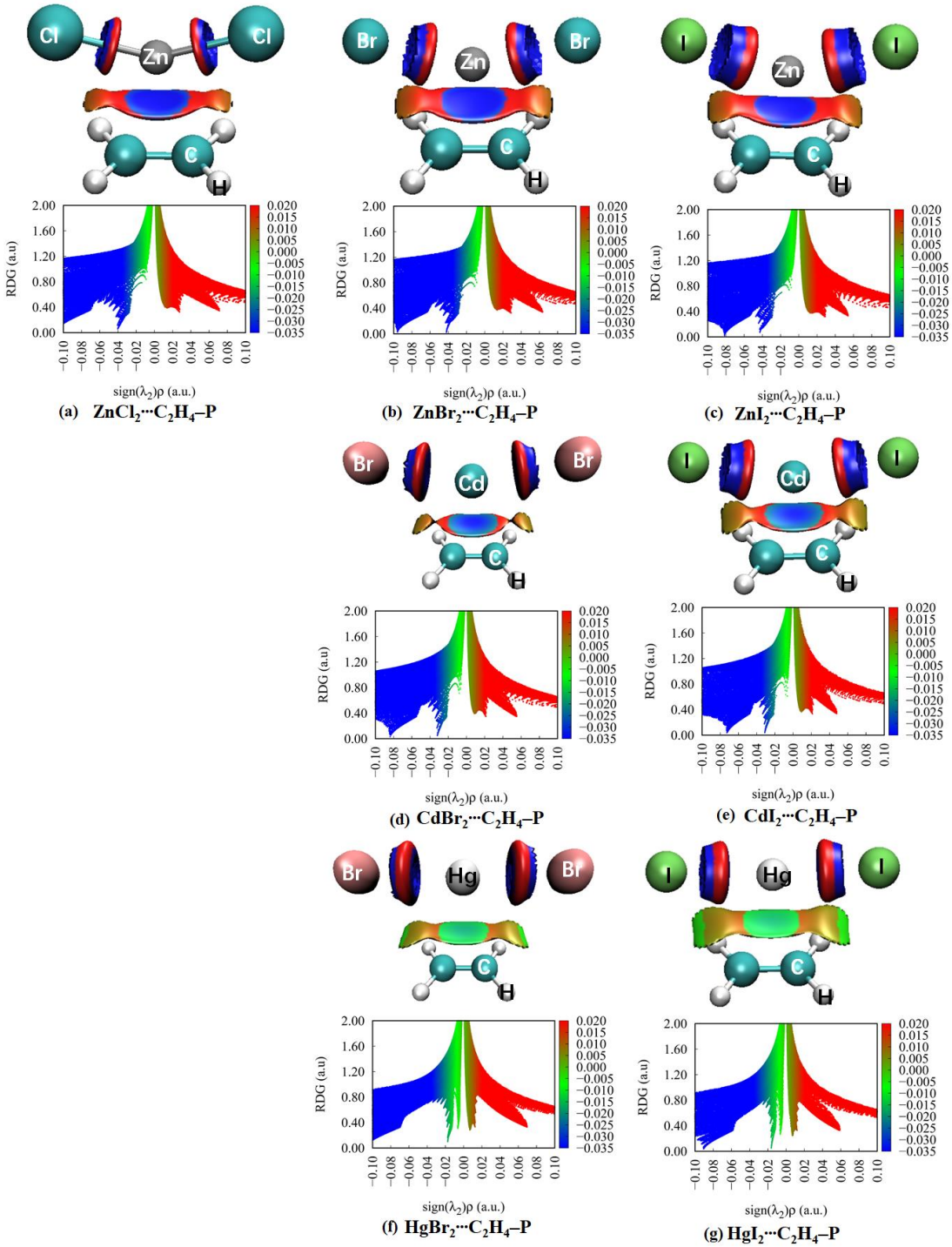

Figure S4. Plots of the reduced density gradient RDG *versus* the electron density multiplied by the sign of the second Hessian eigenvalue (sign(λ_2)ρ) of $MX_2\cdots C_2H_4$–P. NCI maps of the corresponding binary complexes. Blue, green, orange, and red areas correspond to strong attractive, weak attractive, weak repulsive, and strong repulsive interactions, respectively.

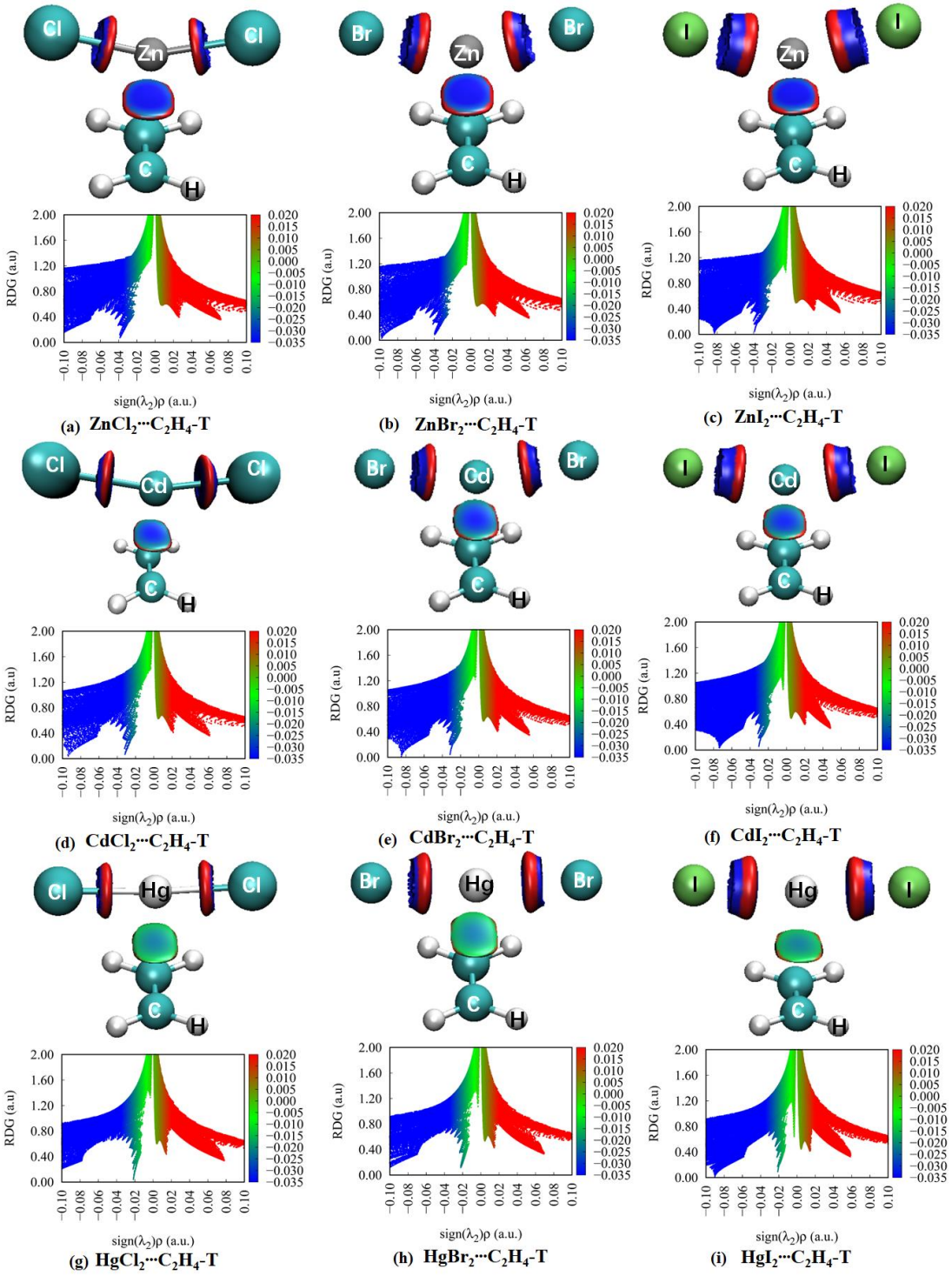

Figure S5. Plots of the reduced density gradient RDG *versus* the electron density multiplied by the sign of the second Hessian eigenvalue (sign(λ_2)ρ) of $MX_2\cdots C_2H_4$–T. NCI maps of the corresponding binary complexes. Blue, green, orange, and red areas correspond to strong attractive, weak attractive, weak repulsive, and strong repulsive interactions, respectively.

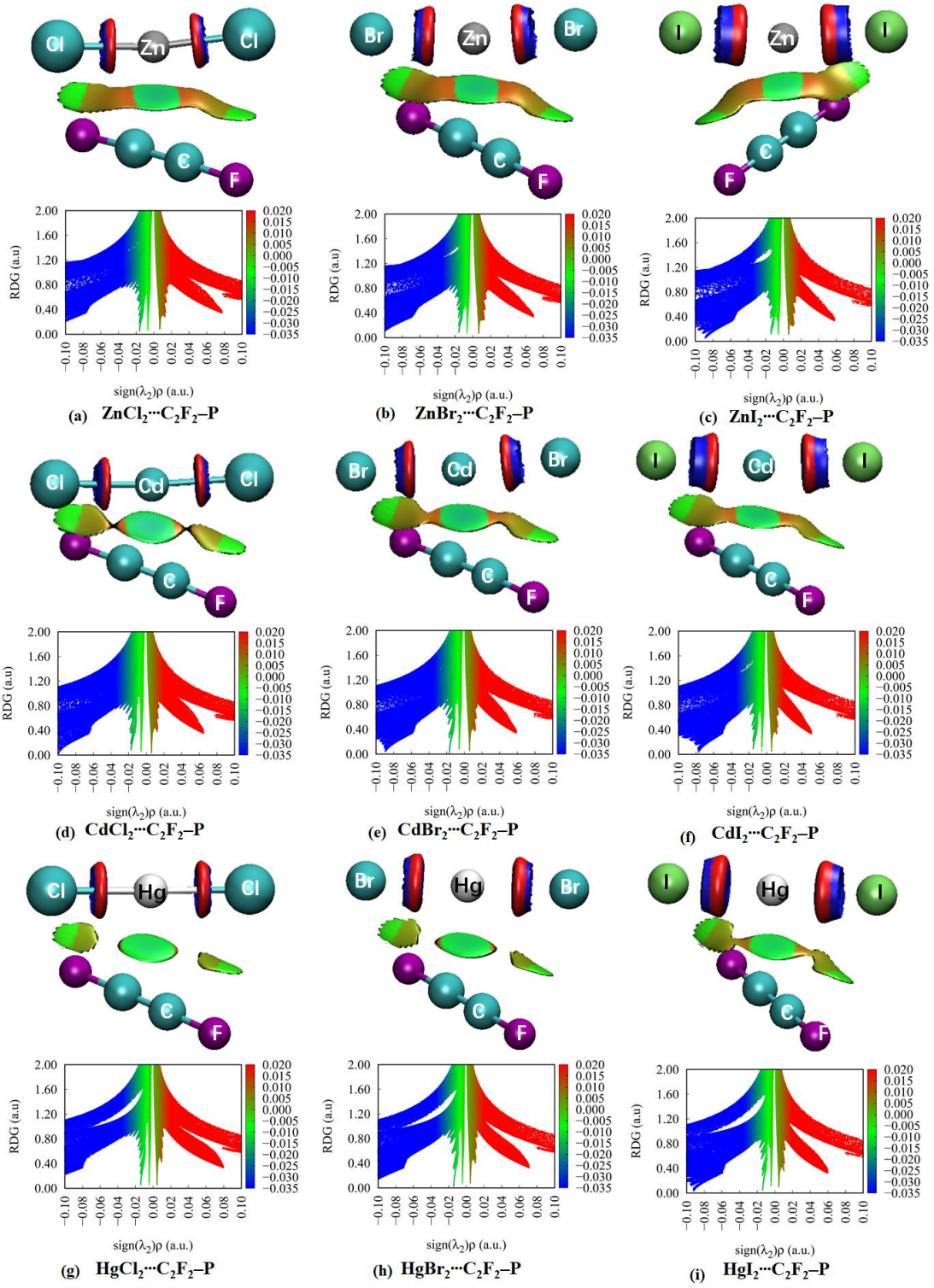

Figure S6. Plots of the reduced density gradient RDG *versus* the electron density multiplied by the sign of the second Hessian eigenvalue (sign(λ_2)ρ) of $MX_2\cdots C_2F_2$–P. NCI maps of the corresponding binary complexes. Blue, green, orange, and red areas correspond to strong attractive, weak attractive, weak repulsive, and strong repulsive interactions, respectively.

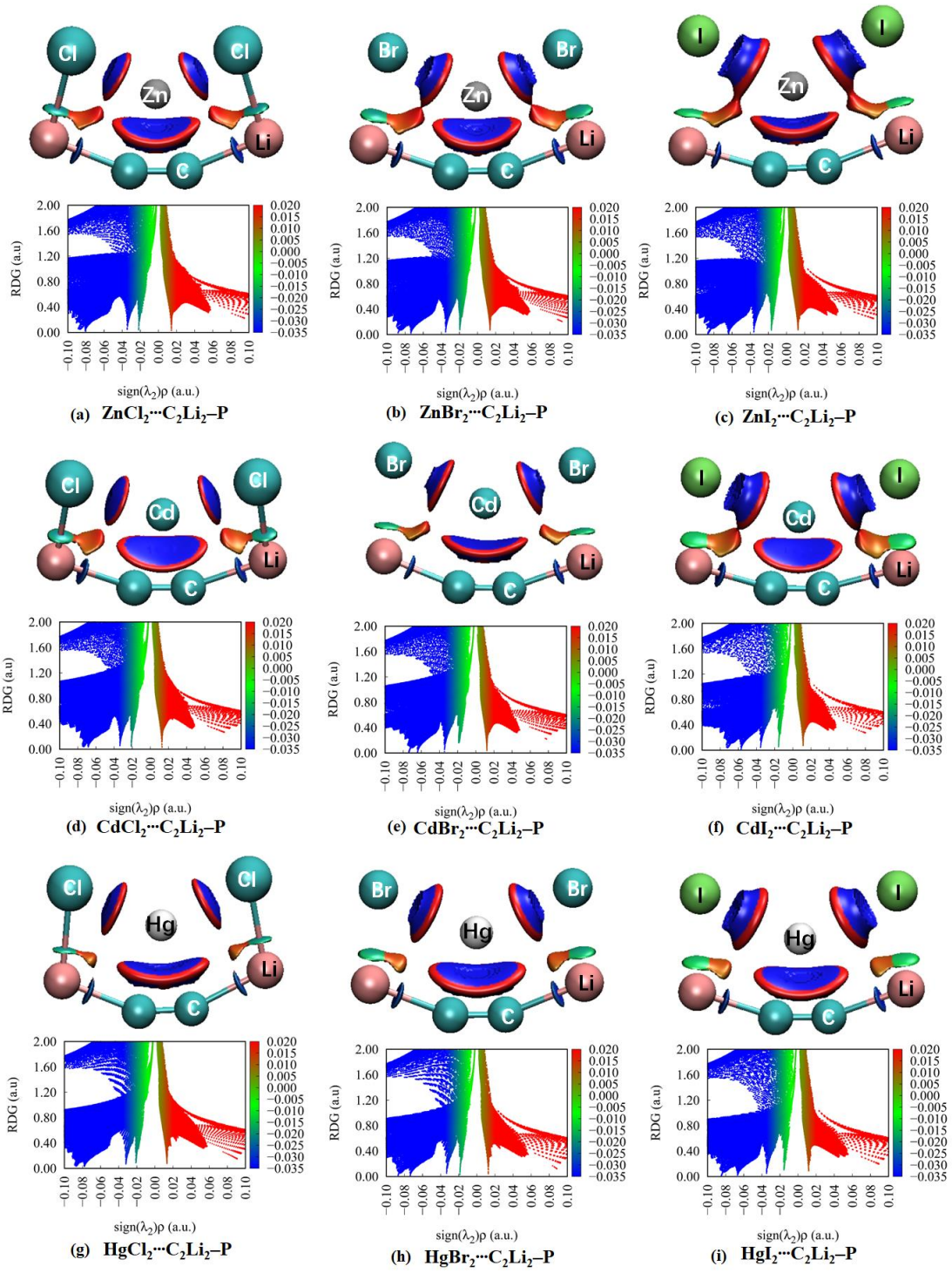

Figure S7. Plots of the reduced density gradient RDG *versus* the electron density multiplied by the sign of the second Hessian eigenvalue (sign(λ_2)ρ) of $MX_2\cdots C_2Li_2$–P. NCI maps of the corresponding binary complexes. Blue, green, orange, and red areas correspond to strong attractive, weak attractive, weak repulsive, and strong repulsive interactions, respectively.

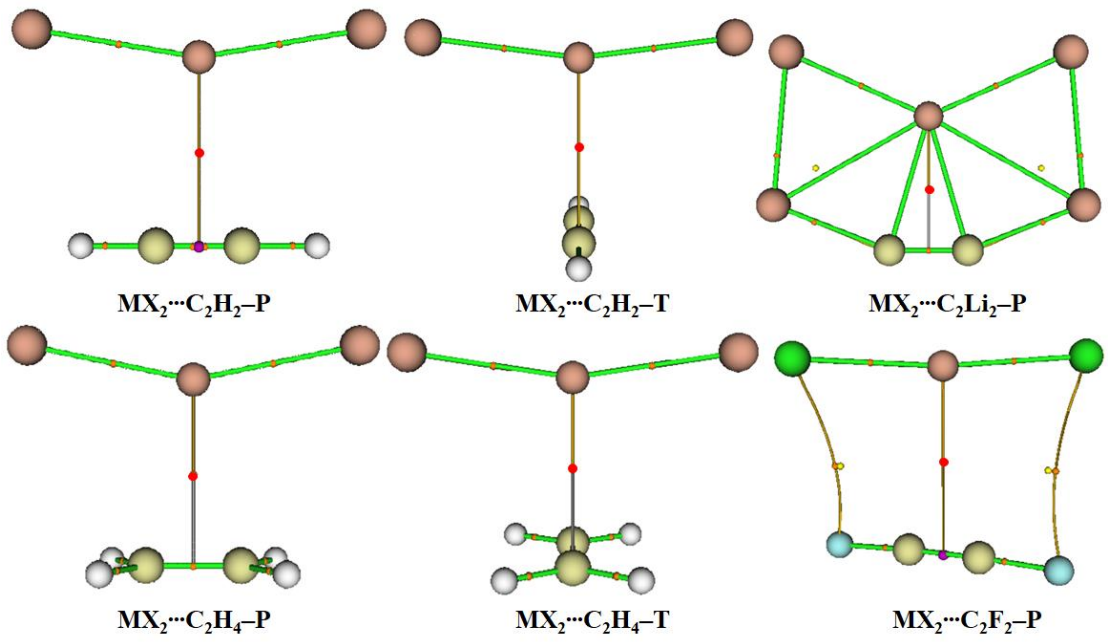

Figure S8. Molecular graphs of spodium–π bonded stable complexes at the intermolecular bond critical points.

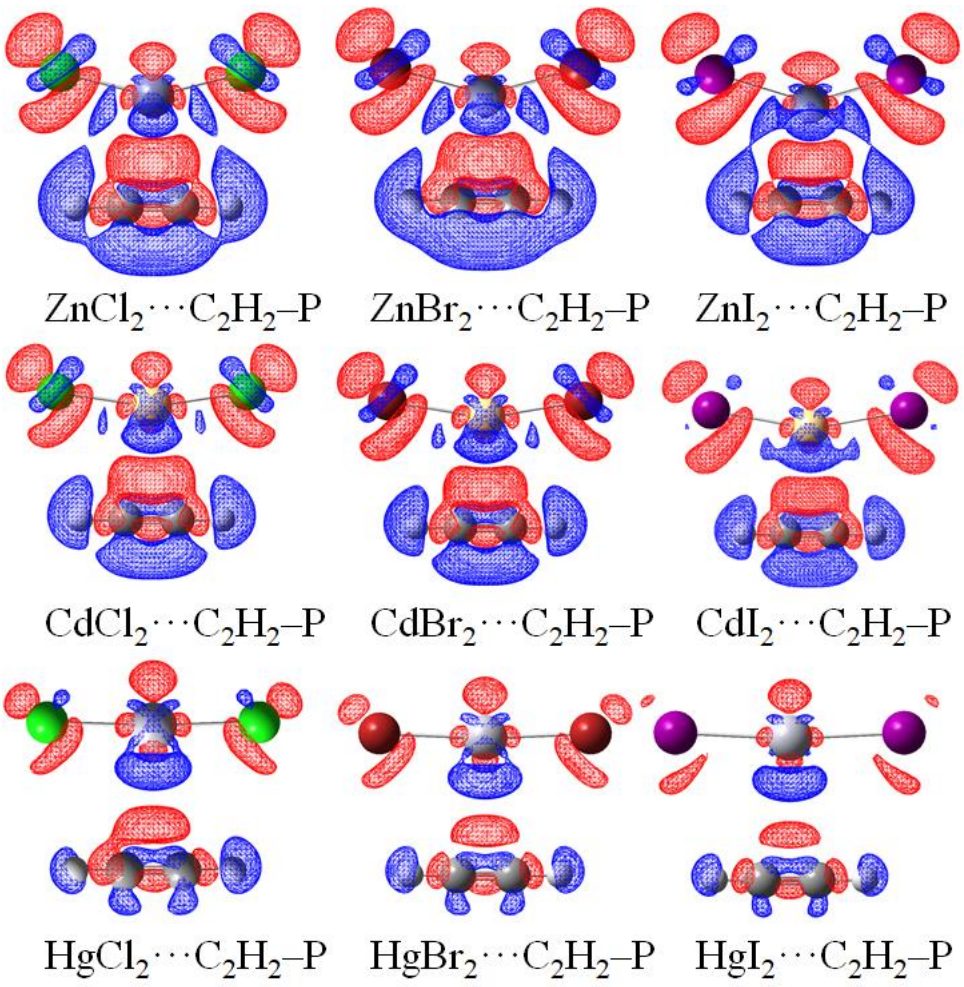

Figure S9. Electron density shifts of the $MX_2\cdots C_2H_2$–P complexes (iso = ± 0.0008). Red regions indicate increased electron density, while blue regions represent decreased electron density.

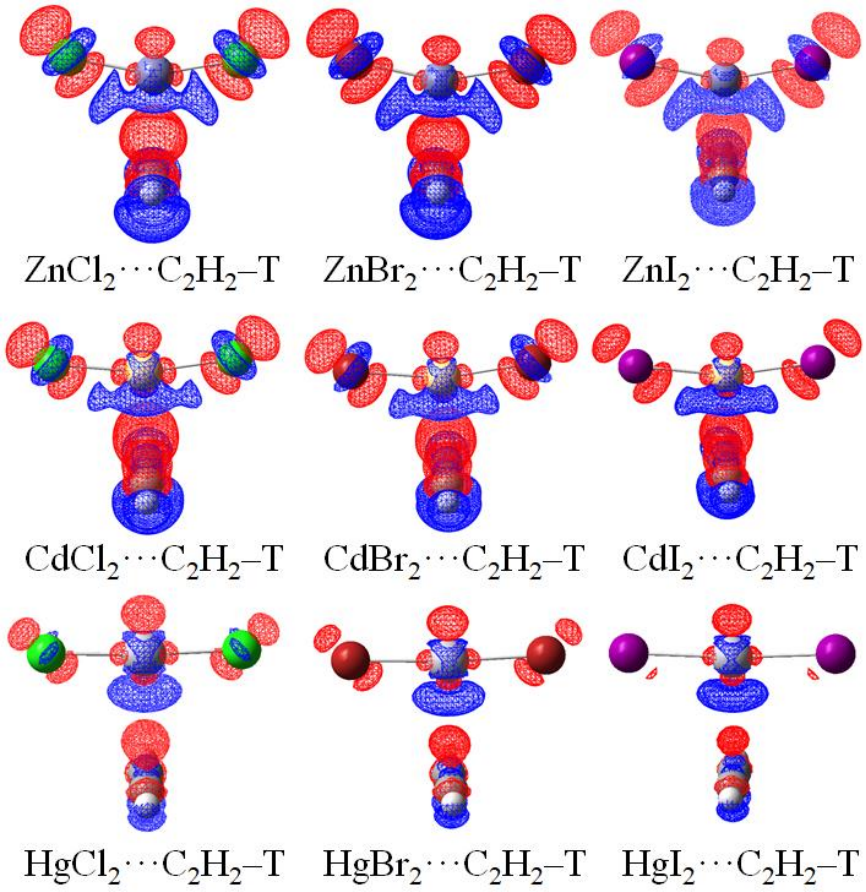

Figure S10. Electron density shifts of the $MX_2\cdots C_2H_2$–T complexes (iso = ± 0.0008). Red regions indicate increased electron density, while blue regions represent decreased electron density.

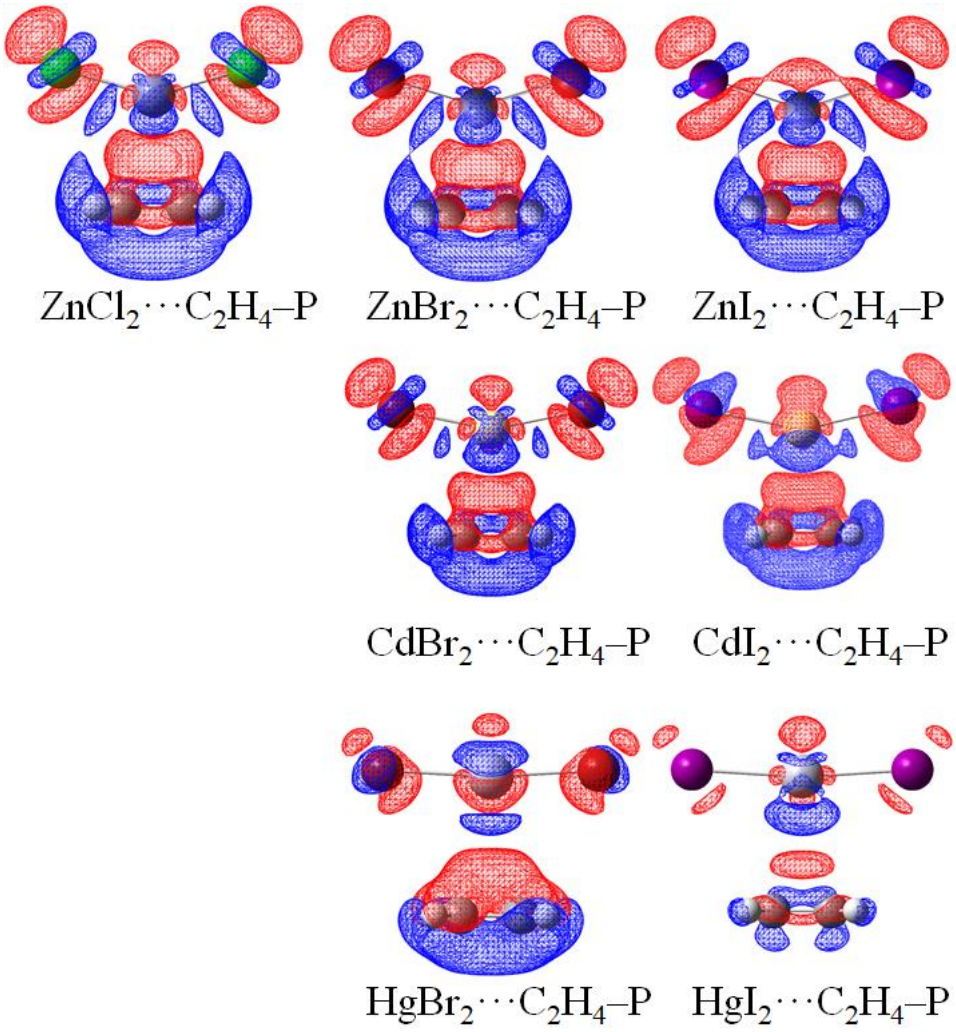

Figure S11. Electron density shifts of the $MX_2\cdots C_2H_4$–P complexes (iso = ± 0.0008). Red regions indicate increased electron density, while blue regions represent decreased electron density.

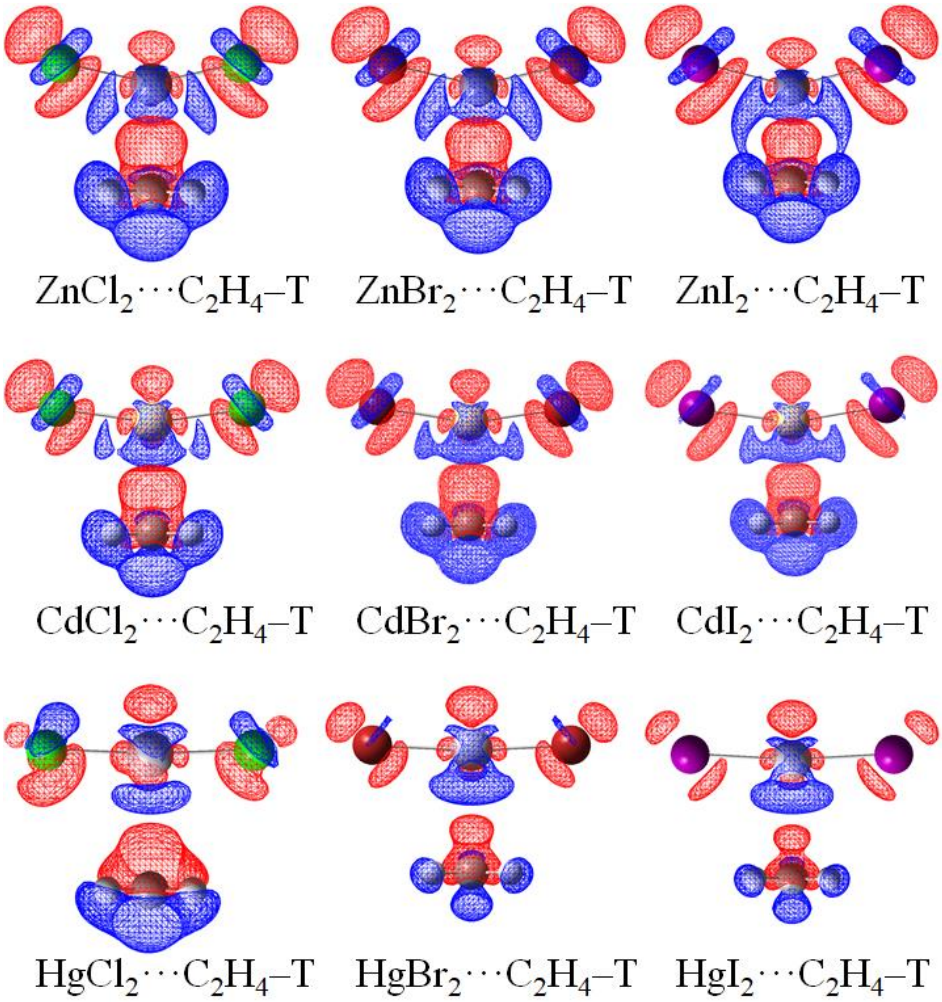

Figure S12. Electron density shifts of the $MX_2\cdots C_2H_4$-T complexes (iso = ± 0.0008). Red regions indicate increased electron density, while blue regions represent decreased electron density.

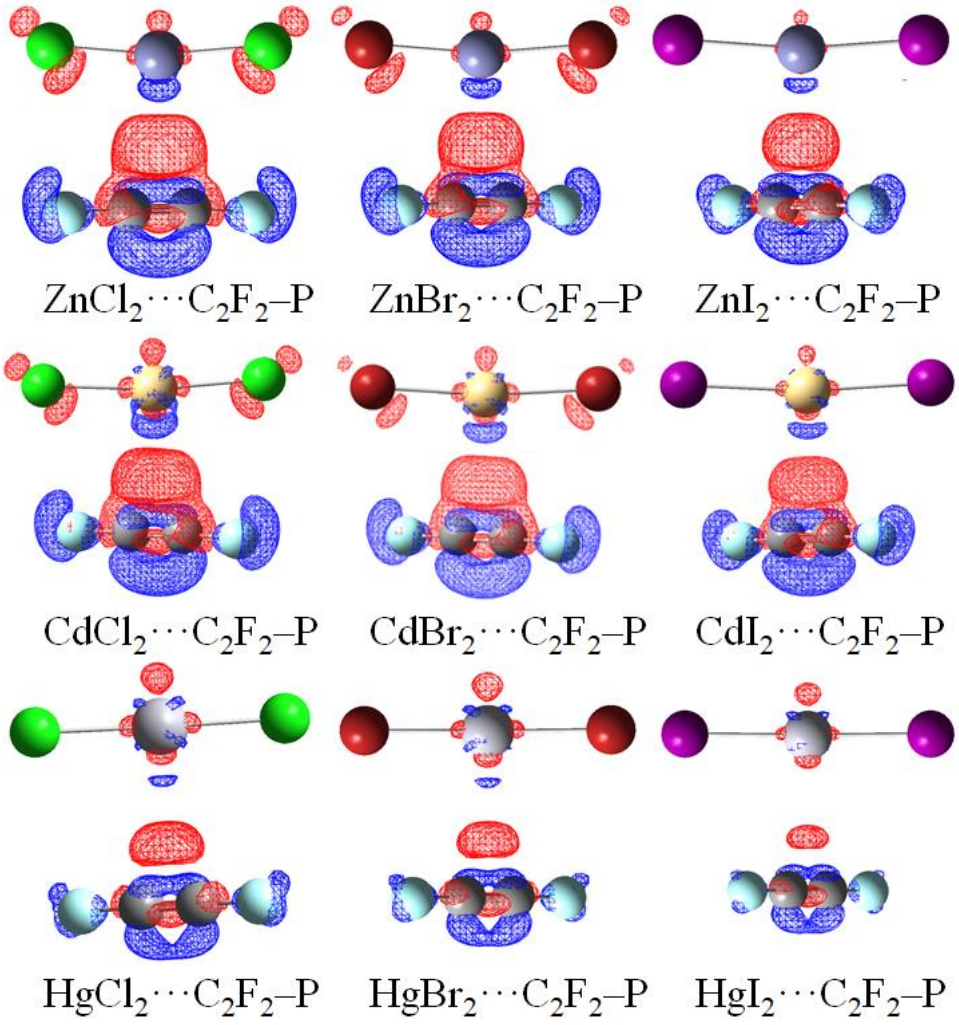

Figure S13. Electron density shifts of the $MX_2\cdots C_2F_2$–P complexes (iso = ± 0.0008). Red regions indicate increased electron density, while blue regions represent decreased electron density.

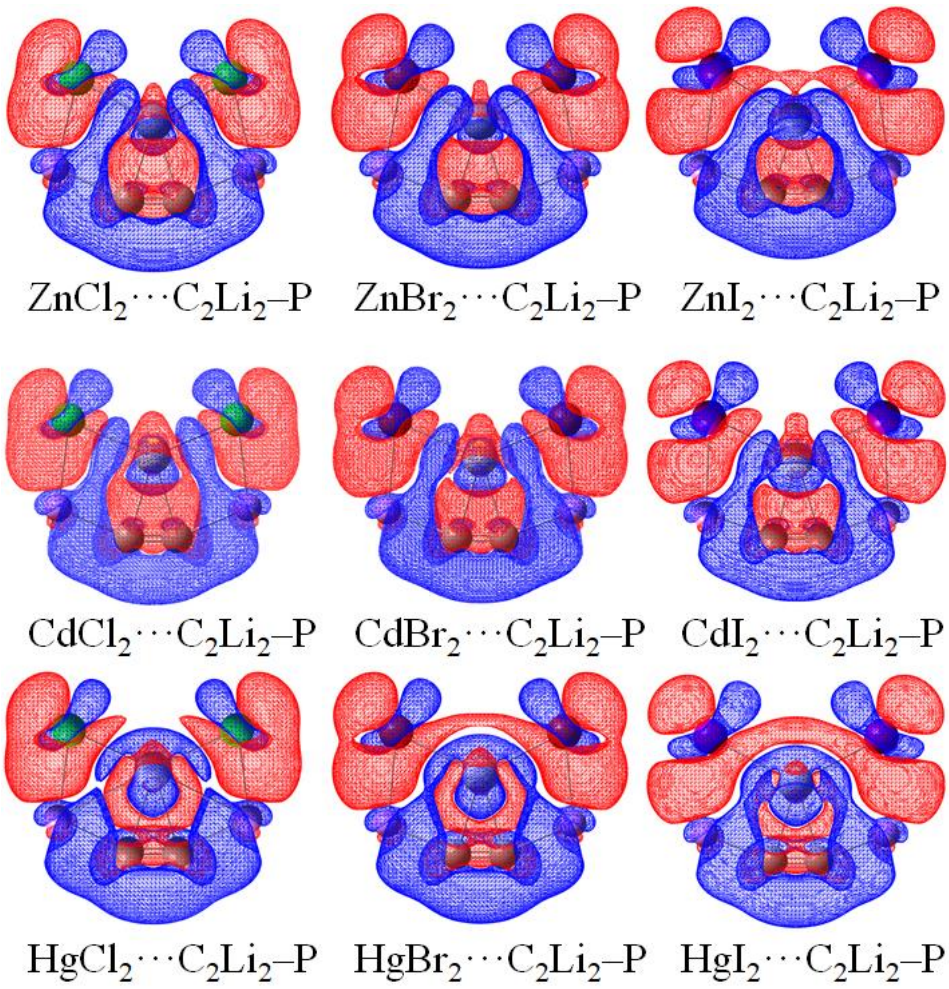

Figure S14. Electron density shifts of the $MX_2\cdots C_2Li_2$–P complexes (iso = ± 0.0008). Red regions indicate increased electron density, while blue regions represent decreased electron density.

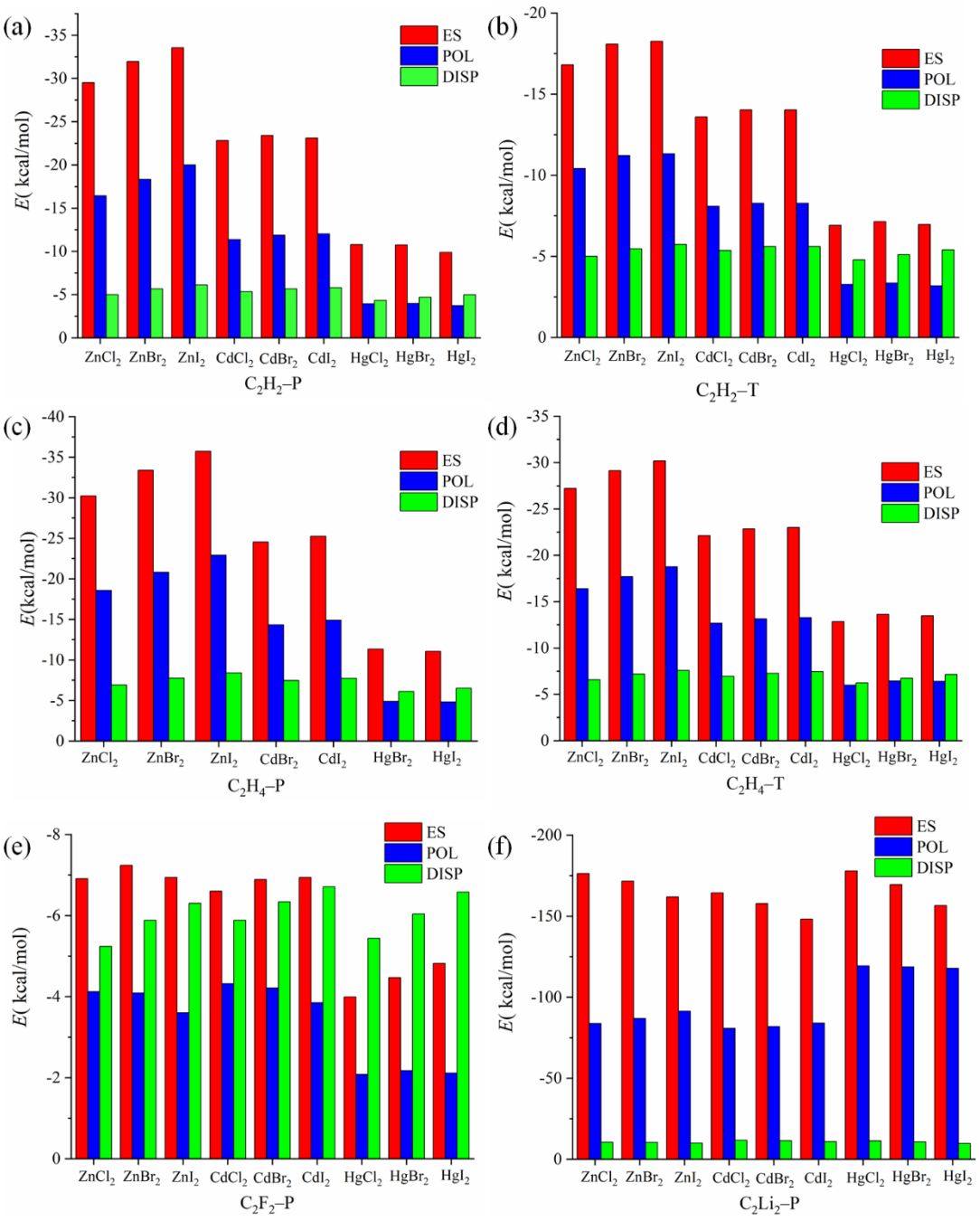

Figure S15. Comparison of electrostatic (ES), polarization (POL), and dispersion (DISP) energies in the binary complexes.